Psychopharmacology
DOI 10.1007/s00213-014-3639-6

ORIGINAL INVESTIGATION

Persistent modification of forebrain networks and metabolism in rats following adolescent exposure to a 5-HT7 receptor agonist

Rossella Canese • Francesca Zoratto • Luisa Altabella • Paola Porcari • Laura Mercurio • Francesco de Pasquale • Erica Butti • Gianvito Martino • Enza Lacivita • Marcello Leopoldo • Giovanni Laviola • Walter Adriani

Received: 28 October 2013 / Accepted: 22 May 2014

Abstract
Rationale The serotonin 7 receptor (5-HT7-R) is part of a neuro-transmission system with a proposed role in neural plasticity and in mood, cognitive or sleep regulation.
Objectives We investigated long-term consequences of sub-chronic treatment, during adolescence (43–45 to 47–49 days old) in rats, with a novel 5-HT7-R agonist (LP-211, 0 or 0.250 mg/kg/day).
Methods We evaluated behavioural changes as well as forebrain structural/functional modifications by in vivo magnetic resonance (MR) in a 4.7 T system, followed by ex vivo histology.
Results Adult rats pre-treated during adolescence showed reduced anxiety-related behaviour, in terms of reduced avoidance in the light/dark test and a less fragmented pattern of exploration in the novel object recognition test. Diffusion tensor imaging (DTI) revealed decreased mean diffusivity (MD) in the amygdala, increased fractional anisotropy (FA) in the hippocampus (Hip) and reduced axial (D||) together with increased radial (D⊥) diffusivity in the nucleus accumbens (NAcc). An increased neural dendritic arborization was confirmed in the NAcc by ex vivo histology. Seed-based functional MR imaging (fMRI) identified increased strength of connectivity within and between "limbic" and "cortical" loops, with affected cross-correlations between amygdala, NAcc and Hip. The latter displayed enhanced connections through the dorsal striatum (dStr) to dorsolateral prefrontal cortex (dl-PFC) and cerebellum. Functional connection also increased between amygdala and limbic elements such as NAcc, orbito-frontal cortex (OFC) and hypothalamus. MR spectroscopy (1H-MRS) indicated that adolescent LP-211 exposure increased glutamate and total creatine in the adult Hip.
Conclusions Persistent MR-detectable modifications indicate a rearrangement within forebrain networks, accounting for long-lasting behavioural changes as a function of developmental 5-HT7-R stimulation.

Keywords Magnetic resonance spectroscopy · DTI · Functional connectivity · Hippocampus · Nucleus accumbens · Amygdala · Limbic loop · Cortical loop · Serotonin 7 receptor · Anxiety

Rossella Canese and Francesca Zoratto contributed equally to this work as co-first authors.

Electronic supplementary material The online version of this article (doi:10.1007/s00213-014-3639-6) contains supplementary material, which is available to authorized users.

R. Canese (✉) · F. Zoratto · L. Altabella · P. Porcari · L. Mercurio · G. Laviola · W. Adriani
Department of Cell Biology and Neurosciences, Istituto Superiore di Sanità, viale Regina Elena 299, Rome 00161, Italy
e-mail: rossella.canese@iss.it

F. de Pasquale
Institute for Advanced Biomedical Technologies, University "G. D'Annunzio", Chieti, Italy

E. Butti · G. Martino
Division of Neuroscience, San Raffaele Scientific Institute, Milan, Italy

E. Lacivita · M. Leopoldo
Dipartimento di Farmacia—Scienze del Farmaco, Università degli Studi di Bari "A. Moro", Bari, Italy

F. Zoratto
Bambino Gesù Children's Hospital IRCCS, Rome, Italy

P. Porcari
Physics Department, Sapienza University of Rome, Rome, Italy

Published online: 13 June 2014

Introduction

The serotonin (5-hydroxytryptamine, 5-HT) 7 receptor (5-HT7-R) has been recently proposed for a role in neurogenesis, synaptogenesis and dendritic spine formation, especially during development (Kobe et al. 2012; Kvachnina et al. 2005). There is increasing interest in this neuro-transmission system because of a possible involvement in learning and memory processes (Cifariello et al. 2008; Sarkisyan and Hedlund 2009) as well as in patho-physiological processes like anxiety/depression or cognitive and sleep disturbances (Bonaventure et al. 2007; Wesolowska et al. 2006). Initially discovered in the supra-chiasmatic nucleus of the hypothalamus and involved in diurnal-nocturnal rhythms of activity (Duncan et al. 2004; Sprouse et al. 2004), this receptor is distributed in the thalamus, hypothalamus and hippocampus, with lower levels in the cerebral cortex and limbic areas (Hedlund 2009; Hedlund and Sutcliffe 2006).

Although 5-HT7-R activation may exert a negative control on 5-HT neural activity, particularly via the dorsal raphe (Duncan et al. 2004) and/or via the medial prefrontal cortex (mPFC), little is currently known about the effects of selective agonist drugs. LP-211 is a novel agonist whose in vitro pharmacological properties make it suitable for possible psychoactive effects (Hedlund et al. 2010; Leopoldo et al. 2011). Pre-clinical evidence in mice and rats demonstrates consistent acute/sub-chronic effects onto exploratory motivation, anxiety-related profiles and spontaneous circadian rhythm (Adriani et al. 2012; Ruocco et al. 2014a, b). 5-HT7-R may have a role in neural plasticity during development; as such, pharmacological 5-HT7-R stimulation may well result in neuro-plastic changes leading to persistent consequences in the brain circuits. The issue of developmental effects originated by sub-chronic exposure to such drugs is as yet unexplored, and a developmental approach is warranted.

In this framework, we previously reported 5-HT7-R mRNA and protein up-regulation in the striatum of adult rats after sub-chronic methylphenidate (MPH) administration during adolescence. This profile was associated with a persistent reduction of impulsive behaviour (Leo et al. 2009). As MPH is an indirect and non-selective monoaminergic agonist, it is possible that long-term effects of adolescent MPH exposure could be mediated, at least in part, by MPH-induced 5-HT7-R up-regulation. It could be proposed that direct agonist action on 5-HT7-R could trigger neuro-plastic adaptations as those elicited by MPH. Therefore, we sought to explore the consequences of direct 5-HT7-R agonist exposure during adolescence at behavioural as well as structural/functional levels in forebrain circuitry. With this aim, we exploited the potential offered by non-invasive in vivo magnetic resonance (MR) techniques.

Diffusion tensor imaging (DTI) allows imaging of neuro-anatomy and neural connectivity without the need of exogenous contrast agents, providing reproducible quantitative measures such as mean diffusivity (MD, describing the diffusivity of water molecules in brain microstructures) and fractional anisotropy (FA, reflecting the anisotropy of grey and white matter) (Mukherjee and McKinstry 2006; Wang and Melhem 2005). The completely non-invasive nature of DTI has easily allowed a translation to clinical use, where it has become a common technique to investigate structural changes in neuro-anatomy (Schaechter et al. 2009; Takao et al. 2010). Beyond being used to study white matter integrity, DTI also provides key information about the immature brain prior to myelination, during maturation, as well as in normal and disease states.

Moreover, the synchronized and low-frequency spontaneous fluctuations of the functional magnetic resonance imaging (fMRI) signal have recently been applied to investigate large-scale neuronal networks of the brain, in the absence of a specific task or challenge (Raichle and Snyder 2007). Although the neural mechanisms underlying these fluctuations remain largely unknown, several recent studies have demonstrated correlations in resting state low-frequency fMRI signal fluctuations in anaesthetized rodents (Kannurpatti et al. 2008; Pawela et al. 2008). We investigated whether the neural rearrangements, thought to occur as a consequence of the developmental 5-HT7-R stimulation, implied a functional change of neuronal network connectivity within drug-targeted forebrain areas.

Here, we investigated the long-term consequences of adolescent sub-chronic exposure to LP-211, with a specific focus on behaviour, anatomical connectivity (by DTI) and functional connectivity (by resting state fMRI). Anxiety-related behaviour was tested in the light/dark test; depressive-like behaviour was evaluated with the forced swim test while episodic-like memory was assessed with the novel object recognition test. Depressive profile and episodic-like memory were both investigated, because of the possible overlap with pre-clinical anxiety manifestations (Razafsha et al. 2013). The amygdala was studied because of the well-known relation with anxiety-related behaviour; all the remaining structures such as the hippocampus (Hip), dorsal/ventral striata (dStr/NAcc) and prefrontal cortex (PFC) were included because of their established relation to the amygdala. We also applied—in the selected brain regions showing adaptations using the above techniques—in vivo proton magnetic resonance spectroscopy (^{1}H MRS, providing a snapshot of the neuro-chemical environment within defined regions of the brain) or ex vivo histology by Golgi staining. The Hip was also chosen since a recent study (Manganas et al. 2007) showed the possibility of detecting neuro-genesis in vivo by analyzing the signal at 1.28 ppm in ^{1}H MR spectra. The NAcc was chosen a posteriori as it is part of the so-called "extended amygdala" and because of peculiar alterations in DTI parameters.

Materials and methods

All experimental procedures were approved by the Italian Ministry of Health (licence to G.L.). Procedures were in agreement with the European Communities Council Directive (86/609/EEC). All efforts were made to minimize suffering, to reduce the number of animals and to utilize alternatives to in vivo techniques.

Subjects

Fifty-six male Wistar-Han rats (Charles River, France) were used in total for this study. Upon arrival (after weaning), animals were housed in pairs inside polycarbonate cages (42.5 × 26.6 × 18.5 cm), in an air-conditioned room (21 ± 1 °C, humidity 60±10 %), with a 12-h light/dark cycle (lights off at 8.00 a.m.). Food ("Altromin-R", A. Rieper SpA, Vandoies, Italy) and tap water were provided ad libitum. Each pair of rats was randomly assigned to receive a subchronic administration with LP-211 (0.250 mg/kg/day i.p., *n*=29) or vehicle (0.5–1 % DMSO in saline, *n*=27) for 5 days during the adolescent phase (Post-Natal Day, PND: 43–45 to 47–49 days old) and tested in adulthood (PND>60 days old) for potential carry-over effects. Drug dose and regimen were chosen according to previous work with mice (Adriani et al. 2012; Romano et al. 2014) and rats (Ruocco et al. 2014a, b). The experiment was run in three cohorts. At adulthood, 20 rats (first cohort) were tested for anxiety with the light/dark test (PND 66–67) and then underwent MR analyses (PND 72–83), with the aim of measuring long-term modifications in relevant brain areas. This first cohort was not used for ex vivo measures. At sacrifice (PND 85), the brains of six rats (second cohort) were prepared for Golgi staining. This second cohort remained untouched after adolescent drug exposure until sacrifice, to avoid any interference on drug-induced changes within forebrain morphology. At adulthood, 30 rats (third cohort) were continuously monitored for spontaneous home cage locomotor activity (PND 84–90) and were then evaluated in the novel object recognition test (PND 91–94) for episodic-like memory and in the forced swim test (PND 105) for depressive-like behaviour.

Behavioural observations

Light/dark test

The experimental apparatus is the same as in Adriani et al. (2010), installed in a soundproof cubicle to minimize any distraction. On the day of testing, rats were brought to the soundproof cubicle and left in their home cages for 30 min to acclimate to the surroundings. Each rat was then gently placed into the middle of the white compartment and left to freely explore the whole apparatus for 15 min (Bourin and Hascoet 2003; Laviola et al. 1992). The floor of the apparatus was cleaned, after each animal testing, with water and ethanol (2:1). Experimental sessions were performed between 10.00 and 16.00, over 2 days (PND 66–67; *N*=20, first cohort), with experimental groups being counterbalanced across days. Time spent in the "lit chamber" (100 lux) is an index of anxiety-related behaviour, as it is known that rodents tend to avoid novel and brightly illuminated areas that can induce an aversive reaction (Laviola et al. 1992).

Circadian cycle

Rats were continuously monitored for spontaneous home cage locomotor activity (Adriani et al. 2012; Zoratto et al. 2013) by means of an automatic device equipped with small passive infrared sensors (20 Hz), placed on a standard rack over the top of each home cage (ActiviScope system; TechnoSmart, Rome, Italy). Activity was continuously measured in LP-211 (*n*=8 pairs) and control (*n*=7 pairs) subjects over 7 days (PND 84–90; *N*=15 pairs, third cohort). From this period, we extracted the central 5-day interval, from which a mean day was calculated.

Novel object recognition test

The novel object recognition test is based upon the tendency of rodents to investigate a novel object rather than a familiar one (Ennaceur and Delacour 1988). Rats (PND 91–94; *N*=14, third cohort) were tested (during the dark phase of the light/dark cycle) in a soundproof experimental room, under dim light conditions. A habituation session to the apparatus (a black Plexiglas box, 80 × 80 × 60 cm) was performed for 3 days, 10 min daily (Freret et al. 2014). On the fourth day, an acquisition session (S1; duration 3 min) was performed with two identical objects (a1 and a2, placed in two adjacent corners, 20 cm from the walls). The animal was placed in the opposite quadrant, facing away from the objects. After an intersession interval (ISI; duration 4 h, the animal was placed in its home cage), the retention session (S2; duration 3 min) was performed. Thus, the testing box (cleaned with 33 % alcohol solution) contained two different objects: a familiar one (identical to that previously explored during acquisition, a3) and a new one (b). The objects were metal bowls (diameter 5–8 cm, 5 cm high, weight 150 g) and glass jars (5×5 cm, 6.5 cm high, weight 150 g). Objects presented during acquisition and the new one presented during retention were randomized between animals and were cleaned between trials with 33 % alcohol solution. Each session was video recorded, and the exploratory behaviour (Bevins and Besheer 2006) was scored using ethological software (Observer 2.0; Noldus, Wageningen, The Netherlands). The pattern of exploration was also considered: *Average duration of single exploration episodes* was calculated by dividing the cumulative time, spent exploring one object, by the number of times exploration of that object was initiated (i.e. total duration/frequency).

Forced swim test

To measure their willingness to escape an aversive inescapable situation, rats (PND 105; N=16, third cohort) were tested on the forced swim test (Porsolt et al. 1977; Cryan et al. 2005). Each rat was placed individually in a container (40.0 ×33.0×51.5 cm) containing 32.5 cm of water at 25± 1 °C. One 9-min swimming test session was videotaped from above and subsequently analyzed using ethological software (Observer 2.0; Noldus, Wageningen, The Netherlands). For behavioural parameters considered, see e.g. Prince et al. (1986).

Statistical analysis of behavioural data

Data were analyzed, using Statview II (Abacus Concepts, CA, USA), by general analysis of variance (ANOVA) or repeated measures ANOVA. The latter was applied on data sets involving comparisons of data collected on the same animals over different time intervals (i.e. circadian cycle, novel object recognition test, forced swim test). Multiple post hoc comparisons were performed, where appropriate, using Tukey's honestly significant difference (HSD) test. Data are expressed as mean±SEM. Level of significance was set at $P \leq 0.05$. All statistics are two-tailed.

Preparation of animals for MRI/MRS protocol

The animals were anaesthetized with 2.5 % isoflurane (Forane, Abbott SpA, Latina, Italy) in oxygen 2 L/min. Once unresponsive to paw pinch, each rat was transferred to a stereotaxic head frame, under the continuous supply of anaesthetic gases; anaesthesia was reduced to 2.0 % isoflurane in oxygen (1 L/min). Rats were left to spontaneously breathe, with no mechanical ventilation, during the whole MR experiment which lasted about 2.5 h on average. All MR experiments were conducted on a 4.7 T Agilent Inova pre-clinical system (Agilent Technologies Inc., Palo Alto, CA, USA) equipped with a combination of volume and surface coils (Rapid Biomedical GmbH, Rimpar, Germany) according to protocols described in Canese et al. (2009, 2012). Gradient echo scout images detected accurate positioning of the head. Fast spin-echo sagittal anatomical images (Repetition Time (TR) / Echo Time (TE)=3,000/60 ms, 15 slices of 1-mm thickness, Field of View (FOV) 40×40 mm^2, matrix 256×256, 2 averages, scan time 12 min) were acquired for positioning of images (DTI and fMRI) and of the voxel (MRS).

DTI protocol

This technique provides information about the microarchitecture of white and grey matter, by parameters such as FA, axial diffusivity (D‖), radial diffusivity (D⊥) and MD. FA is a dimensionless value that allows the detection of directionality regardless of the fibre orientation. It is influenced by a number of factors including axonal myelination, diameter, density and orientational coherence (Alexander et al. 2007; Beaulieu 2002). Axial and radial diffusivities describe water diffusion along and across axonal tracts, respectively. Axonal injury, such as axonal swelling, results in reduced D‖, while de-myelination increases D⊥ (Song et al. 2002; Sun et al. 2006). MD is a measure of the directionally averaged magnitude of diffusion and is related to the integrity of the local brain tissue (Beaulieu 2002).

A spin-echo sequence was used with addition of the Stejskal-Tanner diffusion gradients, applied along six non-collinear directions. Intensity, duration and diffusion time were set to 8.27 G/cm, 8 ms and 25 ms, respectively, given a b value of 700 s/mm^2. A FOVof 25×25 mm^2 was sampled on a 64×64 matrix. Multi-slice DT images were acquired (15 slices, 1-mm thickness) in coronal plane (2 averages, TR/TE= 2,000/50 ms). One data set without diffusion weighting was also acquired (total DTI scan time less than 30 min). For each rat, a manual binary brain mask was used to define parenchyma voxels for further analysis. All data were corrected for eddy current distortions with an affine transformation of the diffusion-weighted images to the non-diffusion-weighted image by means of FDT diffusion toolbox in FMRIB Software Library (FSL) software (http://www.fmrib.ox.ac.uk/fsl/). After eddy current corrections, the diffusion tensor (i.e. a matrix describing the orientation dependence in each voxel) was determined, and the eigenvalues (λ1, λ2 and λ3) and then eigenvectors (V1, V2 and V3) of the diffusion tensors were calculated. From the eigenvectors and eigenvalues, maps of FA (Basser and Pierpaoli 1996) were calculated, describing the anisotropy of diffusion, and directionally encoded colour (DEC) maps were generated. Here the colour of each voxel is defined by the orientation of its primary eigenvector (V1) and the intensity is proportional to FA (Pajevic and Pierpaoli 1999). Finally, maps were also calculated for the following: (a) MD, showing the diffusivity value averaged among the three directions; (b) axial diffusivity (D‖=λ1), showing the diffusivity parallel to the direction of the principal eigenvector; and (c) radial diffusivity (D⊥=(λ2+λ3)/2), describing the diffusivity perpendicular to the principal eigenvector. An in-house MATLAB script (Mathworks, Natick, MA,USA) was used to analyze DTI data by manually selecting specific regions of interest (ROIs) from the FA, MD, D‖ and D⊥ maps. In particular, five different regions of the brain were extracted: the amygdala, the Hip, the NAcc, the dStr and the orbital prefrontal cortex (OFC), as shown in Fig. 1. Location of each ROI was chosen by comparison with rat brain atlas (Paxinos and Watson 1998). Significant differences of FA, MD, D‖ and D⊥ values between groups were assessed by an unpaired two-tailed Student's t test ($P \leq 0.05$).

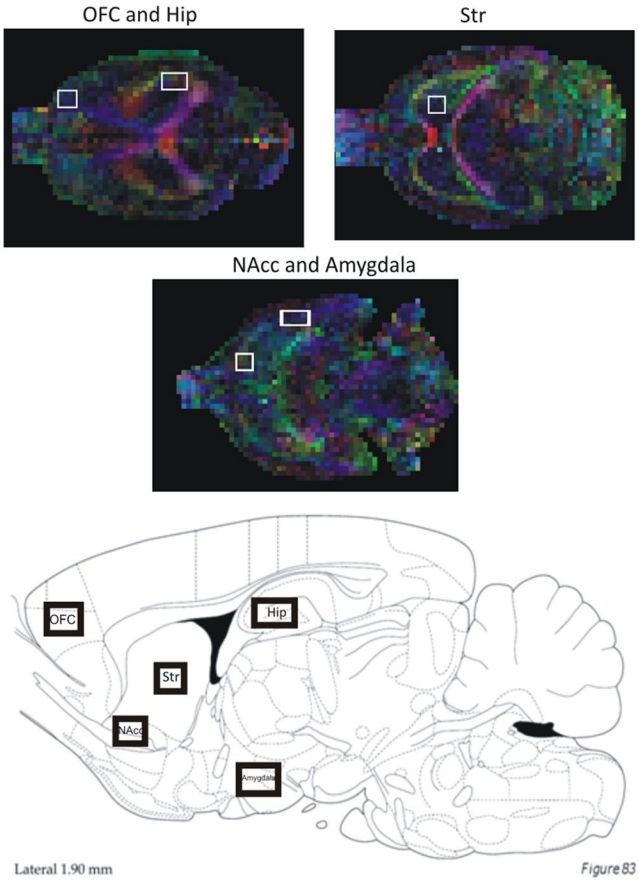

Fig. 1 Examples of in vivo DTI images, with directionally encoded colors (DEC): horizontal (i.e. coronal) maps of rat brains at −3.8, −4.8 and −7.8 mm ventrally from the bregma (Paxinos and Watson 1998). Maps show FA, with color coding the predominant diffusion direction of the anisotropy. *White rectangles* denote the voxel placed on amygdala, Hip, dStr and NAcc, as well as OFC, as shown in the rat brain atlas sagittal diagram (Paxinos and Watson 1998). The overall results are shown in Table 1

Functional connectivity protocol

In resting subjects, there are spontaneous, slow (<0.1 Hz) fluctuations of the blood oxygen level-dependent (BOLD) signal which are temporally coherent within widely distributed functional networks. Our seed-based analysis, based on a bootstrap resampling approach, is able to find a distinct series of "active" voxels in which the cross-correlation to the seed, observed in the template obtained for LP-211-pre-treated animals, differs from the bootstrapping threshold, calculated from resampling of the controls in that same voxel. Therefore, we can obtain clear images of all the surrounding neural networks, connected to that seed.

The fMRI session lasted 30 min, and the MR sequence was a multi-slice sagittal gradient echo sequence (TR/TE=200/5 ms, 7 slices of 2-mm thickness, FOV 30×30 mm^2, 64×64 matrix, 140 temporal points). The acquisition of seven consecutive slices was due to a precise strategy to obtain fMRI signals at the highest-frequency content (that in fMRI is around 0.3 Hz). Such spectral content is adequate for investigating resting state networks that are characterized by a low-frequency content (typically around 0.1 Hz, see for example de Pasquale et al. (2010)). The analysis stream consisted of a pre-processing and then a seed-based statistical approach with a bootstrap resampling technique, both implemented in home-made software (developed in MATLAB). The pre-processing was based on image realignment, to reduce the artifacts due to animal movement (Canese et al. 2009), and temporal smoothing, using a moving average method (span width = 5 temporal points). Those rats showing excessive movement of the head (defined as rapid changes of signal larger than 20 % during the fMRI study) were excluded from the analysis. The number of excluded animals consequently determined the number of animals used for analysis: they were n=7 and n=6 for the adolescent-treated and control groups, respectively. Seed-based resting state fMRI connectivity maps for the two groups of animals were generated as follows. Initially, in order to assess temporal reproducibility for the adolescent-treated animals, the 30-min fMRI session (run without any stimulation) was split into three sub-sessions of 10 min each. Subsequently, ten different seeds were placed on brain images, located in five relevant forebrain areas: amygdala, Hip, NAcc, dStr and OFC in both hemispheres. Then, for each given seed (out of these ten), the correlation between its timecourse and the voxel timecourses from the rest of the brain was computed. This step was performed on each data set individually; therefore, separate correlation maps were obtained for every sub-session of every rat. One template image was generated from these correlation maps for the adolescent-treated group, and a threshold was applied by adopting the statistical values as follows. Correlation maps of control animals were resampled with replacement using bootstrapping (Efron and Tibshirani 1988), in order to assess the data reliability and reproducibility and to set significance threshold for active voxels. Resampling is a powerful technique used in fMRI analysis, in particular, to overcome the problem of the test-retest method (Noll et al. 1997) and/or to assess the significance of activation clustering (Auffermann et al. 2002) using the bootstrap or jackknife method. This resampling was carried out by preserving the spatial information for each voxel. To identify significant changes, the 99th percentile of the resampled data set was computed for each voxel. On the mean template map of adolescent-treated animals, correlations higher than the corresponding threshold (from the resampled control maps) have been labelled as significant changes in connection. The output images index the extent of such change, since algebraic differences between the mean correlation value for the adolescent-treated group and the corresponding threshold value of the same voxel are presented (see Fig. 2). The ten maps, one for each seed, represent the brain regions in which the strength of connection with the seed is significantly higher than controls, due to adolescent LP-211 exposure.

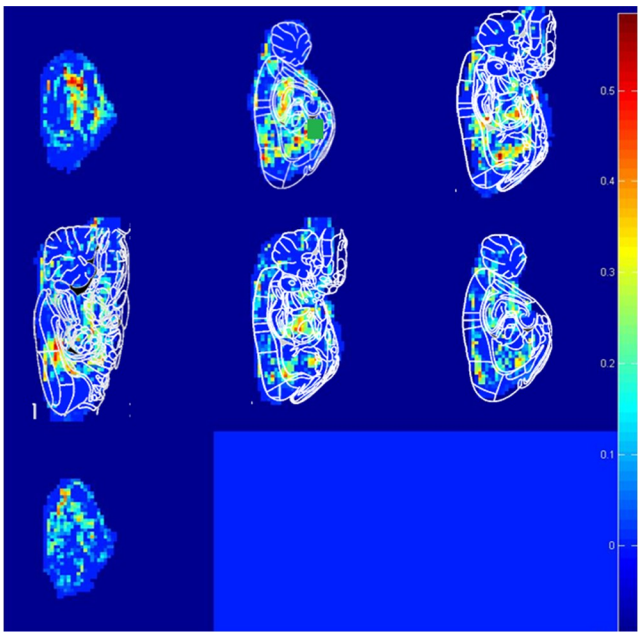

Fig. 2 Voxels showing differences between the correlation maps, related to a particular seed for the adolescent-treated animals, with respect to the threshold (namely, the 99th percentile of the resampled distributions of control animals). As a first step, fluctuations of the blood oxygen level dependent (BOLD) signal allowed generation of a set of individual maps of connectivity for each seed, which were then averaged to obtain one template of adolescent-treated animals for each seed. The sagittal images shown here, obtained with a seed positioned in the right amygdala (*green square*), denote those pixels whose connectivity to the seed was enhanced as a long-term consequence of adolescent LP-211 exposure. Rat brain atlas diagrams (Paxinos and Watson 1998), corresponding to the centre of the MRI slices, are over-imposed to the difference maps. The overall results are shown in Supplementary Fig. 1s and summarized in Table 2

MRS protocol

Single voxel-localized ^{1}H MR spectra (PRESS, TR/TE= 4,000/23 ms, ns=256) were collected from the Hip (volume 33.6 μL) in order to detect metabolite alterations (in particular those related to neurogenesis, by analyzing the signal at 1.28 ppm). A quantitative MRS protocol, including water T2 measurements, was applied (Canese et al. 2012). Localized shimming was performed up to water linewidths ranging between 7 and 10 Hz. Spectra were analyzed using LCModel (Provencher 1993). Metabolite concentrations are expressed in millimole per liter (mM). The effect of treatment on T2 values and metabolite concentrations was assessed using ANOVA with treatment as factor (Statview II, Abacus Concepts, CA, USA). In addition to the 1.28-ppm signal, the following seven metabolites were considered: glutamine (Gln), glutamate (Glu), myo-inositol (Ins), *N*-acetyl-aspartate (NAA), taurine (Tau), sum of glicero-phospho-choline and phospho-choline (GPC+PCh), sum of creatine and phospho-creatine (Cr+PCr). The potential relationship, between those metabolites whose concentrations differed significantly, was then assessed using Pearson linear correlation. Data are expressed as mean±SD. Significance level was set at $P \leq 0.05$.

Stereological analysis of Golgi-stained NAcc neurons

Golgi staining (Izzo et al. 1987) was performed on coronal sections (60-μm thickness) containing striatal neurons from rats of the second cohort (n=3 per group). At sacrifice, the brains were removed from the skulls and entirely immersed in solutions of the Rapid Golgi-Stain Kit (GolgiStain™ by FD NeuroTechnologies, Columbia, MD, USA), following manufacturer instructions. Coronal sections (60 μm) were cut from the chunk of tissue on a cryostat. Medium spiny neurons in the ventral striatum (NAcc) were analyzed by an observer blind to treatment. Five neurons per animal were analyzed by microscopy with a × 100 magnification lens (*Leica*). The randomly chosen neurons were totally and completely impregnated, clearly distinguishable from adjacent cells, and characterized by continuous, unbroken dendrites.

Dendritic branches and spines were traced using Neurolucida 8.0 (MBF Biosciences, Williston, VT, USA) following the structures through the Z axis. Cell tracings were analyzed by Neurolucida Explorer 4.0. The 3D morphometric analysis uses concentric spheres with a distance of 10 μm between each sphere (Sholl 1981). The smallest sphere is centred within the soma. Spine length and spine density were determined using the measuring tool available on the Stereo-Investigator software (MicroBrightField, Inc., Colchester, VT, USA). These morphometric parameters were also estimated using the branch order method (Greenough and Chang 1985). The developmental effect of adolescent treatment on a total of nine morphometric parameters (number of dendrites, number of dendritic intersections, number of spines, total length of dendrites, total surface of dendrites, total volume of dendrites, spine volume, spine length, distance from spine head to dendrite) was determined by a multivariate analysis of variance (MANOVA), due to the potentially high correlation between these dependent variables. Pillai's statistic was used. Univariate ANOVAs were then conducted for each variable (Statview II, Abacus Concepts, CA, USA). Data are expressed as mean±SD. Significance level was set at $P \leq 0.05$.

Results

Light/dark test

Time spent in the lit chamber and latency to enter into the dark chamber Subjects that had been treated during adolescence with LP-211 spent a significantly increased amount of time in the lit chamber compared to controls, revealing a decrease of anxiety-like behaviour (treatment $F_{1,18}$=6.24, P=0.022; Fig. 3, left panel). LP-211-pre-treated subjects showed increased

latencies to perform the first passage into the dark chamber when compared to vehicle (VEH) controls (treatment $F_{1,18}$= 4.54, P=0.047; LP-211 37.60±5.32 s; VEH 22.90±4.39 s).

Other parameters The number of passages between compartments did not differ among groups (LP-211 13.9±4.1; VEH 13.8 ± 4.6; ns). We did not find significant differences in locomotor activity between groups neither in the lit nor in the dark chamber (data not shown). No difference was found in body weight (LP-211 257.9±5.3 g; VEH 265.9±6.2 g; ns).

Circadian cycle

Data collected from the automated ActiviScope system showed that circadian activity patterns were not affected by adolescent pre-treatment, neither in diurnal rest pattern nor in nocturnal activity pattern, with a complete overlap of the expected peaks of activity (data not shown).

Novel object recognition test

Total duration of object exploration As expected, during the acquisition session, subjects spent a comparable time exploring objects a1 and a2 (a1 14.29±1.84 s; a2 16.54±1.85 s; ns). By contrast, during the retention session, they spent a significantly higher amount of time exploring object b compared to a3 (session x object $F_{1,12}$=7.75, P=0.017; a3 14.96±1.54 s; b 25.63 ± 2.44 s), confirming novelty recognition. No pre-treatment-dependent differences emerged (data not shown), suggesting that LP-211 exposure during adolescence did not affect, on the long-term, the episodic-like memory performances as a whole.

Exploration pattern The average duration of single exploration episodes was calculated, by dividing the cumulative time spent exploring one object by the number of times exploration of that object was initiated. During the retention session, the exploration episodes elicited by object b were significantly longer compared to all other objects (session x object $F_{1,12}$= 5.39, P=0.039; acquisition session, a1 1.69±0.15 s; a2 1.97± 0.15 s; retention session, a3 1.91±0.22 s; b 3.24±0.41 s). However, the duration of exploration episodes shown by control rats did not vary across sessions and objects. By contrast, the duration of exploration episodes shown by LP-211-pre-treated subjects depended on the explored object (object x treatment $F_{1,12}$=3.44, P=0.088).

Multiple post hoc analyses revealed that exploration episodes, specifically directed by LP-211-pre-treated subjects towards object b on retention session, were significantly longer compared to both object a3 (the familiar one on retention session, $P \leq 0.01$) and object a2 (same position on acquisition session, $P \leq 0.01$). Such a profile of results was absent in vehicle controls (Fig. 3, right panel). This finding indicates that adolescent LP-211 exposure permanently affected the exploration pattern: a novel object was able to elicit deeper exploration episodes but only in pre-treated subjects, whereas episodes were of a similar duration (and initiated more frequently) in control subjects.

Forced swim test

No pre-treatment-dependent differences emerged in any of the behavioural parameters considered (struggling, LP-211 63.75 ±7.06 s; VEH 58.39±7.31 s; ns; floating, LP-211 102. 25± 7.79 s; VEH 106.02±8.02 s; ns).

DTI analysis

Results of FA, MD, D|| and D⊥ quantitative analyses are reported in Table 1. Data reveal, in the group of LP-211-pre-treated animals, significant long-term changes in the brain regions. Amygdala showed a significant reduction of MD,

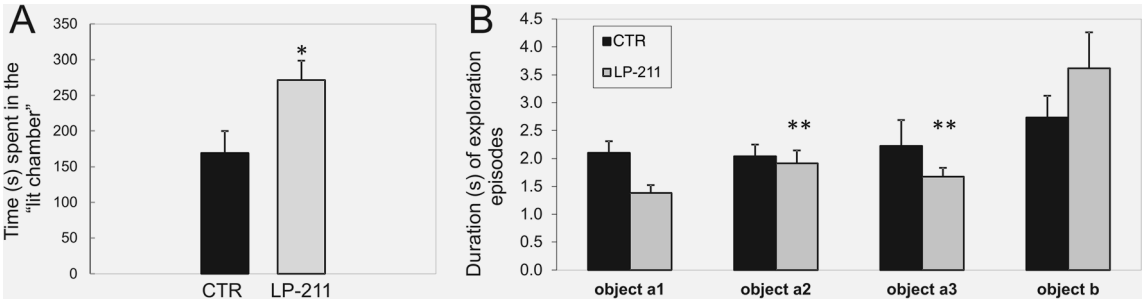

Fig. 3 Anxiety-related behaviour in adult rats (PND>60) that had received a sub-chronic administration with LP-211 (0.250 mg/kg/day i.p.) or vehicle (0.5–1 % DMSO in saline) during adolescence (PND 43–45 to 47–49). a Time spent in the "lit chamber" (100 lux) of a two-side light/dark apparatus (start point lit chamber, single 15-min session). LP-211-pre-treated subjects spent a significantly increased amount of time in the lit chamber (N=20, first cohort). b Exploration pattern (i.e. average duration of single exploration episodes) in the novel object recognition test. Episodes directed towards object b (the novel one on retention session) were significantly longer, compared to both object a3 (the familiar one on retention session) and object a2 (same position on acquisition session), in LP-211-pre-treated but not control subjects (N=14, third cohort). Data are expressed as mean±SEM; (*$P \leq 0.05$; **$P \leq 0.01$) compared to vehicle controls (CTR) or when comparing object b to objects a2 and a3

Table 1 FA, MD, D|| and D⊥ mean values in selected regions. Effects of adolescent LP-211 exposure is denoted by statistically significant differences (*P<0.05) between adolescent-treated and control group (unpaired two-tailed Student's t test). Data are expressed as mean±SD (n=10)

Amygdala	Controls	Treated
FA	0.38±0.12	0.43±0.12
MD (x10^{-3} mm^2/s)	0.84±0.06	0.77±0.05 *
D|| (x10^{-3} mm^2/s)	1.19±0.2	1.09±0.2
D⊥ (x10^{-3} mm^2/s)	0.67±0.06	0.62±0.06 *
Hippocampus (Hip)	Controls	Treated
FA	0.28±0.04	0.43±0.14 *
MD (x10^{-3} mm^2/s)	0.75±0.02	0.76±0.03
D|| (x10^{-3} mm^2/s)	0.97±0.09	1.15±0.11 *
D⊥ (x10^{-3} mm^2/s)	0.67±0.08	0.66±0.05
N.Accumbens (NAcc)	Controls	Treated
FA	0.46±0.08	0.38±0.08
MD (x10^{-3} mm^2/s)	0.79±0.07	0.74±0.04
D|| (x10^{-3} mm^2/s)	1.14±0.09	1.02±0.04 *
D⊥ (x10^{-3} mm^2/s)	0.55±0.03	0.59±0.03 *
Dorsal Striatum (dStr)	Controls	Treated
FA	0.36±0.04	0.37±0.07
MD (x10^{-3} mm^2/s)	0.73±0.02	0.74±0.05
Orbital pre-frontal cortex (OFC)	Controls	Treated
FA	0.44±0.06	0.46±0.06
MD (x10^{-3} mm^2/s)	0.76±0.062	0.70±0.04

due to changes in D⊥. A significant increase of FA was found within the Hip, due to an increase in axial (D||) but not radial (D⊥) diffusivity. No effects were found within the dStr nor the NAcc. However, the NAcc showed a significant decrease in axial together with an increase in radial diffusivity.

Changes in connectivity within the limbic/cortical loop

We detected an increase in the strength of connectivity between some of the seeds, placed a posteriori, and specific voxels in the brain. The complete set of images is shown in Supplementary Materials while one representative example (with the seed positioned in the amygdala, see green square) is shown in Fig. 2. Here, as a long-term consequence of adolescent LP-211 treatment, we observed an increased connectivity of the amygdala to the contralateral NAcc, as well as the following surrounding regions: the ipsilateral dStr, the ipsilateral Hip, both ipsilateral and contralateral thalami. Interestingly, only connection to right ipsilateral Hip was reciprocal (i.e. the ipsilateral amygdala was identified back with a seed placed on the right Hip); only connection to contralateral NAcc and ipsilateral dStr was specular (i.e. results were replicated for two seeds located in symmetric regions of opposing hemispheres). The overall results are summarized in Table 2, listing those regions where changes in connectivity were observed (for seeds located in a given region).

Moreover, Hip and dStr showed the most evident and bilaterally specular changes. The former showed a markedly enhanced connectivity to the ipsilateral Hip (namely, to hippocampal regions surrounding the seed itself), as well as to the ipsilateral and contralateral dStr. The latter, interestingly, was found to show an enhanced connectivity to the ipsilateral prefrontal cortex (PFC) as well as to the contralateral frontal (motor) cortex. Notably, all these connections were bilaterally specular (i.e. replicated for two seeds located in symmetric regions of opposing hemispheres), yet not reciprocal (i.e. increased connectivity was found from the seed to the target regions, but the seed region was not returned when a seed was placed in the target region).

Interestingly, if we follow these unidirectional cross-correlations, we argue that resting state fluctuations apparently cross the hemispheres repeatedly: namely, from the (right) amygdala to the (left) NAcc and then to the (right) dStr; from the (left) amygdala bilaterally through the superior Collicolus/Tectum to OFC and hence to medial hypothalamus; from the (right) Hip to the (left) dStr, then to both (right and left) dorsolateral PFC as well as to the (left) cerebellum. All these regions do identify limbic and cortical loops (see "Discussion"). In addition, the connections of the right Hip turned out to be reciprocal: both contralateral NAcc and ipsilateral amygdala—specifically—were detected among target regions (with enhanced connection) for a Hip seed; consistently, upon positioning of the seed on either of them, the Hip itself was detected in turn.

MRS analysis in the hippocampus

The MRS investigation provided evidence of long-term metabolic changes in the Hip as a consequence of adolescent LP-211 exposure (see Fig. 4). No significant differences, however, were detected in the 1.28-ppm signal, a putative marker of neurogenesis in vivo (see "Discussion"). Water T2 analyses confirmed that no changes occurred in the T2s between the groups (the T2s being 60±2 and 59±2 ms in adolescent-treated vs control Hip, respectively; P=0.38). Glutamate and total creatine concentration were significantly increased in the Hip of adult rats exposed to LP-211 when adolescent ($F_{1,17}$= 12.38, P=0.003 and $F_{1,17}$=6.70, P=0.019, respectively). No treatment-dependent differences emerged for the remaining five metabolites. The individual levels of glutamate and total creatine were then correlated using Pearson linear correlation. A strong positive correlation emerged between the two metabolites (R=0.641; threshold = 0.575 for α=0.01 and N=19).

Stereological analysis of Golgi staining

Compared with control animals, neurons of the LP-211-pretreated rats exhibited a series of clear-cut long-term modifications along the whole extent of the dendrites, as shown in

Table 2 Summary of brain regions showing an increase in the strength of connectivity. Brain regions listed are those which exhibit a significant increase in the strength of connectivity to the seed, depending on its placement in either hemisphere. The template cross-correlation map for that seed, originating from LP-211-pre-treated rats, was compared with the threshold, calculated from control rats after resampling with a bootstrap approach

Seed Placed in:	Right lobe	Left lobe
Amygdala	- contralateral NAcc, ipsilateral dorsal Striatum - ipsilateral Hippocampus (mutual) - ipsi and contralateral Thalamus - lateral cerebellum	- contralateral NAcc, ipsilateral dorsal Striatum - contralateral Amygdala - ipsi and contralateral Superior Colliculus / Tectum
Hippocampus (Hip)	- ipsi and contralateral Hippocampus - ipsi and contralateral Striatum / N.Accumbens (mutual) - ipsi and contralateral Amygdala and internal capsula	- ipsilateral Hippocampus - ipsi and contralateral (dorsal) Striatum (mutual) - contralateral Thalamus and hypothalamus
N.Accumbens (NAcc)	- cortex (spread regions) - ipsi and contralateral (dorsal) Striatum	- contralateral midbrain - contralateral Hippocampus (mutual) - contralateral Striatum/N.Accumbens
Orbital pre-frontal cortex (OFC)	- ipsilateral Superior Colliculus / Tectum - Medial hypothalamus - Medial pre-frontal cortex - ipsi and contralateral internal capsula	- ipsilateral Superior Colliculus / Tectum - Medial pre-frontal cortex
Dorsal Striatum (dStr)	- ipsi and contralateral pre-frontal cortex (dorso-lateral) - contralateral frontal (motor) cortex - contralateral cerebellum (anterior) and Hippocampus (mutual) - ipsi and contralateral Thalamus	- ipsi and contralateral pre-frontal cortex (dorso-lateral) - contralateral frontal (motor) cortex - contralateral Striatum - ipsilateral cerebellum - mid, ipsi and contralateral Thalamus

Fig. 5. The MANOVA revealed a significant main effect of treatment (Pillai's Trace $F_{9,20}$=2.74, P=0.029). Univariate tests showed significant main effects for number of dendritic intersections (+34.8 %, $F_{1,28}$=12.61, P=0.001), number of spines (+38.4 %, $F_{1,28}$=9.36, P=0.005), total length of dendrites (+36.4 %, $F_{1,28}$=9.50, P=0.005), total surface of dendrites (+40.3 %, $F_{1,28}$=10.21, P=0.003), total volume of dendrites (+44.4 %, $F_{1,28}$=9.84, P=0.004) and distance from the spine head to dendrite (+26.55 %, $F_{1,28}$=5.71, P=0.024) in neurons of LP-211 compared to vehicle-pre-treated rats. A tendency towards a significant main effect was also found for spine length ($F_{1,28}$=3.32, P=0.079). No treatment-dependent differences emerged for number of dendrites and spine volume. Comparable results were observed with Sholl analysis, in which a specific dendritic segment (the first 100 μm from soma) of each dendrite was analyzed (data not shown).

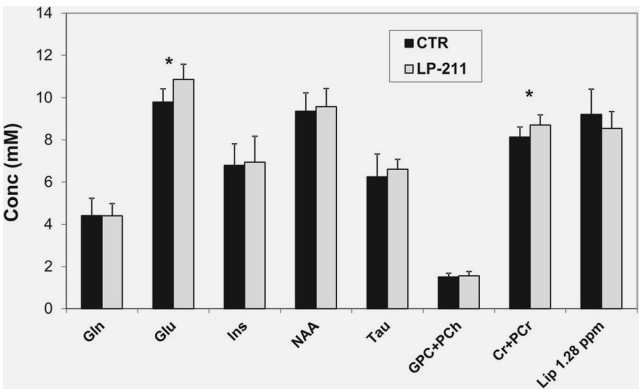

Fig. 4 Metabolite concentrations obtained from in vivo ^{1}H spectra, collected from the hippocampal voxel, by using a quantitative protocol (which uses water as internal standard) and LCModel fitting program. Metabolite assignments: glutamine (Gln), glutamate (Glu), myo-inositol (Ins), *N*-acetyl-aspartate (NAA), taurine (Tau), sum of glicero-phospho-choline and phospho-choline (GPC+PCh), sum of creatine and phospho-creatine (Cr+PCr), lipids (Lip 1.28 ppm). Data are expressed as mean± SD; (*$P \leq 0.05$, **$P \leq 0.01$) compared to controls (CTR)

Discussion

We report plastic rearrangements within forebrain regions and networks as a long-term consequence of a developmental 5-HT7-R stimulation, using a battery of MR analyses. In addition, to confirm suggestions from MR analyses, in a second cohort of rats, we studied morphology (by ex vivo histology) in the NAcc. As far as behaviour is concerned, adult rats that had received a developmental LP-211 exposure during adolescence spent, in a light/dark apparatus, an increased amount of time in the lit chamber (known to be perceived as highly aversive) and showed higher latencies to escape from it. In the novel object recognition test, control animals explored the novel object for longer cumulative time, as expected (Ennaceur and Delacour 1988). This, by means of an increased number of exploration episodes, whose mean duration was the same of those episodes directed towards the familiar object. Thus, as expected in controls, the novel object elicited an approach-avoidance conflict: a drive to explore the unfamiliar object is present, but at the same time, the novelty itself generates a certain degree of anxiety. Such a neophobic behaviour is thought to reflect an animal's fear of novelty

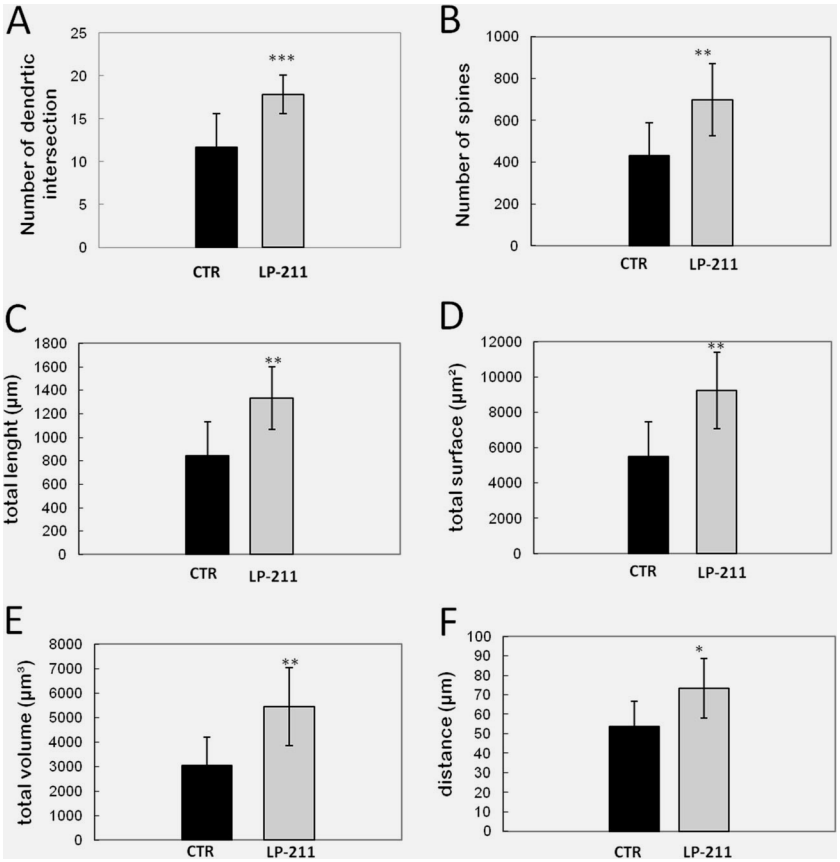

Fig. 5 Effects of adolescent exposure to LP-211 on NAcc neurons of adult rats. LP-211 administration induced an increase in the number of dendritic intersections (a), number of spines (b), total length of dendrites (c), total surface of dendrites (d) and total volume of dendrites (e), along the whole extent of the dendrites; the distance from spine head to dendrite was also significantly increased (f). Data are expressed as mean±SD; (*$P \leq 0.05$, **$P \leq 0.01$, ***$P \leq 0.001$) compared to controls (CTR)

(Brown 2002). As a result, the novelty-exploration pattern in itself remains fragmented. Anxiety is often characterized by repeated transitions from ongoing behaviours (e.g. exploration, feeding) to escape (flight) or other defensive behaviours (Steimer 2011). Similarly, LP-211-pre-treated animals explored the novel object for longer cumulative time. However, the number of exploration episodes directed towards the new object did not increase. This, because the mean duration of each exploration episode was consistently longer. Such a profile suggests carry-over consequences in subjects that had been treated during adolescence with LP-211. The latter group was apparently less affected by the anxiety-inducing component, intrinsic to the new object. As a result, their exploration pattern was much less fragmented. This interpretation is in agreement with the less anxious profile, obtained for LP-211-pre-treated subjects in the light/dark test.

DTI study: structural adaptation in the limbic circuitry (amygdala, Hip and NAcc)

The DTI approach provides clear evidence of plastic rearrangements in brain structures and circuitries for LP-211 compared to vehicle-pre-exposed animals. The increase in FA values reported for the Hip was driven primarily by an increased axial diffusivity, with no change in the radial diffusivity. This finding shall be compared with previous evidence showing an increase in FA, which correlated with histologically verified axonal plasticity during post-injury remodelling (Laitinen et al. 2010). Enhanced axial diffusivity may suggest increased number or calibre of axonal prolongations, a notion that may well fit with the hypothesis of both increased Hip function and enhanced Hip connections to the amygdala, dStr and NAcc (see below). Regarding the amygdala, the reduction of MD (mainly due to decreased radial diffusivity) may suggest an increased number of cells (Blumenfeld-Katzir et al. 2012) and/or increased dendritic arborization. Present changes in DTI (reduced MD) and behaviour (reduced anxiety) appear in agreement with a recent work (Juranek et al. 2012) reporting a relationship between MD and anxiety levels in a pediatric population.

On the other side, data indicate a reduction in axial diffusivity within the NAcc, together with an increase in radial diffusivity. This picture is opposite to what observed within the amygdala and the Hip. Since FA and MD were almost unaffected, it is unlikely that changes in the gross number of cells occurred. A more complex micro-structural remodelling (such as dendritic spines in neural cells and/or of prolongations in glial cells) is thus suggested. An increase in the extent of dendritic arborization was confirmed in ex vivo samples

(see below). This increased arborization is consistent with increased radial diffusion of water.

Morphometric analysis in the NAcc and effects of adolescent exposure to LP-211

A long-lasting increase was identified for LP-211-pre-treated rats in the length of dendrites, in the number of intersections, together with alterations in spine size on the medium spiny neurons (the major output cells of the NAcc). These data are in agreement with the increased spherical geometry of water diffusion in this region, detected in vivo by the DTI approach (see above). Plastic changes in the brain are characterized by alterations in patterns of synaptic connectivity. Function of the 5-HT7-R system is involved in the regulation of neuronal structure in the striatal area (Kvachnina et al. 2005), underlying neuro-behavioural adaptive responses (Hyman et al. 2006; Kelley 2004). Indeed, agonist-induced activation of endogenous 5-HT7-R increases neurite length in striatal neuron cultures (Leo et al. 2009; Speranza et al. 2013). We report here, accordingly, a plastic neuronal remodelling, as a consequence of selective pharmacological stimulation of the 5-HT7 receptor during a developmental window (van Praag et al. 2000).

Long-lasting neuronal modifications are involved in learning processes and/or adaptive recovery of behavioural functions that can persist for long time (Robinson and Kolb 1997). Furthermore, many studies have demonstrated that complex environments and learning experiences in rodents can increase the length of dendrites as well as the density of dendritic spines, and can produce changes in patterns of synaptic connectivity (Kolb et al. 1998; van Praag et al. 2000; Withers and Greenough 1989). Interestingly, quite opposite results were found with amphetamine (Kolb et al. 2003). The ability of experience to alter the dendritic structure is generally considered advantageous and is thought to be the primary mechanism by which past experience influences subsequent behaviour (Kolb et al. 1998). This notion is relevant since, in the present experiment, all rats were housed during adolescence in enriched, stimulating, complex and changing environment. Therefore, we conclude that adolescent exposure to LP-211 induced dendritic arborization and a persistent change in spine's morphology, possibly via a potentiation of the effects induced by experience-dependent plasticity, which was still evident within the NAcc of adult animals.

fMRI connectivity study: changes within the limbic loop

Resting state fMRI signals have been proposed to represent synchronous spontaneous fluctuations of large-scale brain networks (Vincent et al. 2007) that occur at low frequencies. Spontaneous fluctuations were detected in isoflurane-anaesthetized rats with a magnitude of ~2 %, fully comparable to the drug-induced BOLD signal found previously under similar anaesthetic conditions (Canese et al. 2009). Bilateral patterns of connectivity have been so far observed by applying seed-based analysis under various anaesthetic regimens (Herman et al. 2011; Kannurpatti et al. 2008; Pan et al. 2011; Pawela et al. 2009; Wilson et al. 2011).

In our hands, persistent changes appeared as a consequence of developmental LP-211 exposure. Such enhancement identifies well-known forebrain circuits including ventral striatum (NAcc), amygdala, OFC and hypothalamus (limbic loop) as well as Hip, dStr, medial / dorso-lateral PFC and cerebellum (cortical loop). Such circuits have been demonstrated to support affective versus motor/executive functions, respectively (Alexander et al. 1990). Some elements of the limbic loop showed changes in strength of their individual connections to the cortical loop: noteworthy, the OFC showed increased connectivity to the medial PFC; the NAcc also showed increased connectivity to the dStr both directly and indirectly through the Hip; direct mutual changes in connections between amygdala and Hip were detected. All these data point (i) to the amygdala as a central region to the limbic loop, being in turn connected to the other limbic regions and (ii) to the Hip as a central region to the cortical loop, being in turn connected to the other executive motor regions.

Noteworthy, the function of these limbic areas (NAcc, OFC) may be directly regulated by the activity of 5-HT7-R. Indeed, in our recent phMRI study, an increased BOLD signal within these brain areas was induced by administration of the selective 5-HT7-R antagonist, SB-269970 (Canese et al. 2011). It is possible to hypothesize that 5-HT7-R-targeting drugs may tap onto the limbic loop directly, as suggested by the present as well as by our previous study (Canese et al. 2011), and that rearrangement of the cortical loop is an indirect adaptation.

How can developmental 5-HT7-R stimulation change the network connections?

It is known that neuronal activity can reorganize neuronal circuits and connections (Maletic-Savatic et al. 1999) and that, beyond acting as a neurotransmitter, serotonin (5-HT) may also modulate neurite outgrowth and synaptogenesis (Udo et al. 2005). Accordingly, 5-HT7-R activation promotes hippocampal neurite outgrowth (Kvachnina et al. 2005), as well as an increase of dendritic protrusions (Kobe et al. 2012) and an elevation of spinogenesis. 5-HT is an obvious candidate for subserving plasticity of synaptic contacts (Gould 1999). Intriguingly, together with 5-HT1A receptors, 5-HT7 ones are critical in the developing PFC (Beique et al. 2004). Therefore, present findings suggest that pharmacological stimulation of 5-HT7-R during a still plastic developmental window may (i) generate persistent changes in the adult morphology of the limbic loop as well as (ii) strengthen the connectivity to, and within, the cortical loop. Further work is

warranted to ascertain whether the present results could extend to other developmental phases.

MRS study indicating metabolic Hip changes

The finding of increased Glu and increased Cr+PCr suggests enhanced hippocampal function. Glu levels might regulate the excitatory synaptic tone, thus allowing a better contribution to the neural information processing. Conversely, increased levels of total creatine (i.e. Cr+PCr) may provide hippocampal neurons with higher energetic resources (Marco et al. 2007). It has been recently shown that activation of 5-HT7-R accounts for the 5-HT7-mediated effects on hippocampal-related learning (Costa et al. 2012; Eriksson et al. 2008; Gasbarri et al. 2008). Behavioural processes mediated by the Hip, such as (spatial) learning and memory, are improved as a persistent consequence of developmental LP-211 exposure (Ruocco et al. 2014a). It has also been reported that 5-HT7-R stimulation impairs short-term memory, while improving long-term memory (Meneses et al. 2008; Meneses 2014). The suggestion is that memory acquisition requires silencing, while consolidation requires activation of 5-HT7-R (Horiguchi et al. 2011; Perez-Garcia and Meneses 2005, 2009; Sarkisyan and Hedlund 2009; Waters et al. 2012).

Methodological limitations

All the MR techniques present limitations. First, DTI is a direct measure of water diffusion; therefore, changes in DTI parameters are not specific markers, so that any hypothesis about structural effects of a given drug treatment should be confirmed by histology. Functional connectivity is a fairly recent technique, not yet widely employed in animal studies, where anaesthetic regimen can be an important confounding factor. Finally, localized MRS requires a priori choice of the investigated region and can reveal and quantify only those metabolites which are relatively abundant (i.e. present at millimolar concentration).

Another limitation of MR studies is the work effort and cost per each subject, hampering the possibility of several drug dosages, of comparison with other drugs and/or reference compounds, and of comparing more than just one age phase in developmental studies. Drug dosage was chosen based on studies from our group, whereby the LP-211 appeared the most promising among new 5-HT7-R agonists (Leopoldo et al. 2011; Adriani et al. 2012); the 0.250 mg/kg dose was more effective compared to others (Ruocco et al. 2014a, b). The age stage of adolescence was investigated as it models an important turning point for humans, during which many neuropsychiatric disorders may emerge (Laviola et al. 2003; Marco et al. 2007).

Conclusion

We propose that the limbic loop is under developmental, modulatory control of, among others, the 5-HT7-R system (Canese et al. 2011; Romano et al. 2014). As a consequence of the developmental exposure to LP-211, we provide evidence of a rearrangement within forebrain: (i) altered diffusion due to increased dendritic arborization and number of spines within the NAcc; (ii) enhanced connection in neural networks, centered by the amygdala/NAcc as well as Hip/dStr; (iii) a potentiated metabolic activity of the Hip.

It is not possible to completely exclude that LP-211 could also act on 5-HT1A receptors, considering that low micromolar affinity has been reported (Costa et al. 2012; Hedlund et al. 2010) and that 5-HT1A and 5-HT7 receptors may heterodimerize (Renner et al. 2012; Herrick-Davis 2013). The clear-cut behavioural effects on anxiety-related behaviour as well as the MR results for the amygdala would be in agreement with the notion that LP-211 could partially act on 5-HT1A receptors (De Vry 1995). Enduring modifications, however, should in turn reflect over other profiles of behaviour, including disinhibition, sensation seeking (Ruocco et al. 2014b), lower vulnerability to semi-automatic habits (Romano et al. 2014) and potentiated spatial memory (Ruocco et al. 2014a; Freret et al. 2014).

Acknowledgments Research performed under "NeuroGenMRI" (ERA-net "PrioMedChild"), Italian Ministry of Health (Italian partner, grant to W.A.; EU coordinator: L. Reneman); partially funded from "Gambling", Department of Antidrug Policies c/o Presidency of the Council of Ministries, Italy (grant to G.L. and W.A.) and from "EMTICS" (Seventh Framework Programme FP7/2007-2013), agreement no 278367 (Animal Model partner, grant to G.L.). We acknowledge Dr. Flavia Chiarotti for stimulating discussion on bootstrap statistical analyses; Mr. Massimo Giannini for the excellent maintenance of the MR equipment; Dr. Nadia Francia for all management issues; Miss Neha Patel and Miss Saira Shamsi (in ERASMUS stage) for practical support; Mrs. Luigia Cancemi and Mr. Giovanni Dominici for animal care. There is no conflict of interest to disclose.

References

Adriani W, Boyer F, Leo D, Canese R, Podo F, Perrone-Capano C, Dreyer J-L, Laviola G (2010) Social withdrawal and gambling-like profile after lentiviral manipulation of DAT expression in rats' accumbens. Int J Neuro-Psycho-Pharmacol 20:1–14

Adriani W, Travaglini D, Lacivita E, Saso L, Leopoldo M, Laviola G (2012) Modulatory effects of two novel agonists for serotonin receptor 7 on emotion, motivation and circadian rhythm profiles in mice. Neuropharmacology 62:833–842

Alexander GE, Crutcher MD, DeLong MR (1990) Basal ganglia-thalamocortical circuits: parallel substrates for motor, oculomotor, "prefrontal" and "limbic" functions. Prog Brain Res 85:119–146

Alexander AL, Lee JE, Lazar M, Field AS (2007) Diffusion tensor imaging of the brain. Neurotherapeutics 4:316–329

Auffermann WF, Ngan SC, Hu X (2002) Cluster significance testing using the bootstrap. Neuroimage 17:583–591

Basser PJ, Pierpaoli C (1996) Microstructural and physiological features of tissues elucidated by quantitative-diffusion-tensor MRI. J Magn Reson B 111:209–219

Beaulieu C (2002) The basis of anisotropic water diffusion in the nervous system - a technical review. NMR Biomed 15:435–455

Beique JC, Campbell B, Perring P, Hamblin MW, Walker P, Mladenovic L, Andrade R (2004) Serotonergic regulation of membrane potential in developing rat prefrontal cortex: coordinated expression of 5-hydroxytryptamine (5-HT)1A, 5-HT2A, and 5-HT7 receptors. J Neurosci 24:4807–4817

Bevins RA, Besheer J (2006) Object recognition in rats and mice: a one trail non-matching-to sample learning task to study "recognition memory". Nat Protoc 1:1306–1311

Blumenfeld-Katzir T, Pasternak O, Dagan M, Assaf Y (2012) Diffusion MRI of structural brain plasticity induced by a learning and memory task. PLoS ONE 6:e20678

Bonaventure P, Kelly L, Aluisio L, Shelton J, Lord B, Galici R, Miller K, Atack J, Lovenberg TW, Dugovic C (2007) Selective blockade of 5-hydroxytryptamine (5-HT)7 receptors enhances 5-HT transmission, antidepressant-like behavior, and rapid eye movement sleep suppression induced by citalopram in rodents. J Pharmacol Exp Ther 321:690–698

Bourin M, Hascoet M (2003) The mouse light/dark box test. Eur J Pharmacol 463:55–65

Brown GW (2002) Social roles, context and evolution in the origins of depression. J Health Social Behav 43:255–276

Canese R, Adriani W, Marco EM, De Pasquale F, Lorenzini P, De Luca N, Fabi F, Podo F, Laviola G (2009) Peculiar response to methylphenidate in adolescent compared to adult rats: a phMRI study. Psychopharmacology (Berl) 203:143–153

Canese R, Marco EM, De Pasquale F, Podo F, Laviola G, Adriani W (2011) Differential response to specific 5-Ht(7) versus whole-serotonergic drugs in rat forebrains: A phMRI study. Neuroimage 58:885–894

Canese R, Pisanu ME, Mezzanzanica D, Ricci A, Paris L, Bagnoli M, Valeri B, Spada M, Venditti M, Cesolini A, Rodomonte A, Giannini M, Canevari S, Podo F, Iorio E (2012) Characterisation of in-vivo ovarian cancer models by quantitative 1H magnetic resonance spectroscopy and diffusion-weighted imaging. NMR Biomed 25:632–642

Cifariello A, Pompili A, Gasbarri A (2008) 5-HT(7) receptors in the modulation of cognitive processes. Behav Brain Res 195:171–179

Costa L, Spatuzza M, D'Antoni S, Bonaccorso CM, Trovato C, Musumeci SA, Leopoldo M, Lacivita E, Catania MV, Ciranna L (2012) Activation of 5-HT7 serotonin receptors reverses metabotropic glutamate receptor-mediated synaptic plasticity in wild-type and Fmr1 knockout mice, a model of Fragile X syndrome. Biol Psychiatry 72:924–933

Cryan JF, Valentino RJ, Lucki I (2005) Assessing substrates underlying the behavioral effects of antidepressants using the modified rat forced swimming test. Neurosci Biobehav Rev 29(4–5):547–569

de Pasquale F, Della Penna S, Snyder AZ, Lewis C, Mantini D, Marzetti L, Belardinelli P, Ciancetta L, Pizzella V, Romani GL, Corbetta M (2010) Temporal dynamics of spontaneous MEG activity in brain networks. Proc Natl Acad Sci U S A 107:6040–6045

De Vry J (1995) 5-HT1A receptor agonists: recent developments and controversial issues. Psychopharmacology (Berl) 121:1–26

Duncan MJ, Grear KE, Hoskins MA (2004) Aging and SB-269970-A, a selective 5-HT7 receptor antagonist, attenuate circadian phase advances induced by microinjections of serotonergic drugs in the hamster dorsal raphe nucleus. Brain Res 1008:40–48

Efron B, Tibshirani R (1988) An Introduction to the Bootstrap. Boca Raton CRC Press

Ennaceur A, Delacour J (1988) A new one-trial test for neurobiological studies of memory in rats. 1: Behavioral data. Behav Brain Res 31: 47–59

Eriksson TM, Golkar A, Ekstrom JC, Svenningsson P, Ogren SO (2008) 5-HT7 receptor stimulation by 8-OH-DPAT counteracts the impairing effect of 5-HT(1A) receptor stimulation on contextual learning in mice. Eur J Pharmacol 596:107–110

Freret T, Paizanis E, Beaudet G, Gusmao-Montaigne A, Nee G, Dauphin F, Bouet V, Boulouard M (2014) Modulation of 5-HT7 receptor: effect on object recognition performances in mice. Psychopharmacology (Berl) 231(2):393–400

Gasbarri A, Cifariello A, Pompili A, Meneses A (2008) Effect of 5-HT(7) antagonist SB-269970 in the modulation of working and reference memory in the rat. Behav Brain Res 195:164–170

Gould E (1999) Serotonin and hippocampal neurogenesis. Neuropsychopharmacology 21:46S–51S

Greenough WT, Chang F-LF (1985) Synaptic structural correlates of information storage in mammalian nervous systems, Synaptic plasticity. Guilford, New York, pp 335–372

Hedlund PB (2009) The 5-HT7 receptor and disorders of the nervous system: an overview. Psychopharmacology (Berl) 206:345–354

Hedlund PB, Sutcliffe JG (2006) 5-HT7 receptors as favorable pharmacological targets for drug discovery. In: Roth BL (ed) The Serotonin Receptors: From Molecular Pharmacology to Human Therapeutics. Humana Press, Totowa, pp 517–535

Hedlund PB, Leopoldo M, Caccia S, Sarkisyan G, Fracasso C, Martelli G, Lacivita E, Berardi F, Perrone R (2010) LP-211 is a brain penetrant selective agonist for the serotonin 5-HT(7) receptor. Neurosci Lett 481:12–16

Herman P, Sanganahalli BG, Hyder F, Eke A (2011) Fractal analysis of spontaneous fluctuations of the BOLD signal in rat brain. Neuroimage 58:1060–1069

Herrick-Davis K (2013) Functional significance of serotonin receptor dimerization. Exp Brain Res 230(4):375–386

Horiguchi M, Huang M, Meltzer HY (2011) The role of 5-hydroxytryptamine 7 receptors in the phencyclidine-induced novel object recognition deficit in rats. J Pharmacol Exp Ther 338:605–614

Hyman SE, Malenka RC, Nestler EJ (2006) Neural mechanisms of addiction: the role of reward-related learning and memory. Annu Rev Neurosci 29:565–598

Izzo PN, Graybiel AM, Bolam JP (1987) Characterization of substance P- and [Met]enkephalin-immunoreactive neurons in the caudate nucleus of cat and ferret by a single section Golgi procedure. Neuroscience 20:577–587

Juranek J, Johnson CP, Prasad MR, Kramer LA, Saunders A, Filipek PA, Swank PR, Cox CS Jr, Ewing-Cobbs L (2012) Mean diffusivity in the amygdala correlates with anxiety in pediatric TBI. Brain Imaging Behav 6:36–48

Kannurpatti SS, Biswal BB, Kim YR, Rosen BR (2008) Spatio-temporal characteristics of low-frequency BOLD signal fluctuations in isoflurane-anesthetized rat brain. Neuroimage 40:1738–1747

Kelley AE (2004) Memory and addiction: shared neural circuitry and molecular mechanisms. Neuron 44:161–179

Kobe F, Guseva D, Jensen TP, Wirth A, Renner U, Hess D, Muller M, Medrihan L, Zhang W, Zhang M, Braun K, Westerholz S, Herzog A, Radyushkin K, El-Kordi A, Ehrenreich H, Richter DW, Rusakov DA, Ponimaskin E (2012) 5-HT7R/G12 signaling regulates neuronal morphology and function in an age-dependent manner. J Neurosci 32:2915–2930

Kolb B, Forgie M, Gibb R, Gorny G, Rowntree S (1998) Age, experience and the changing brain. Neurosci Biobehav Rev 22:143–159

Kolb B, Gorny G, Li Y, Samaha AN, Robinson TE (2003) Amphetamine or cocaine limits the ability of later experience to promote structural plasticity in the neocortex and nucleus accumbens. Proc Natl Acad Sci U S A 100:10523–10528

Kvachnina E, Liu G, Dityatev A, Renner U, Dumuis A, Richter DW, Dityateva G, Schachner M, Voyno-Yasenetskaya TA, Ponimaskin EG (2005) 5-HT7 receptor is coupled to G alpha subunits of

heterotrimeric G12-protein to regulate gene transcription and neuronal morphology. J Neurosci 25:7821–7830
Laitinen T, Sierra A, Pitkanen A, Grohn O (2010) Diffusion tensor MRI of axonal plasticity in the rat hippocampus. Neuroimage 51:521–530
Laviola G, Dell'Omo G, Alleva E, Bignami G (1992) Ontogeny of cocaine hyperactivity and conditioned place preference in mice. Psychopharmacology (Berl) 107:221–228
Laviola G, Macrì S, Morley-Fletcher S, Adriani W (2003) Risk-taking behavior in adolescent mice: psychobiological determinants and early epigenetic influence. Neurosci Biobehav Rev 27(1–2):19–31
Leo D, Adriani W, Cavaliere C, Cirillo G, Marco EM, Romano E, di Porzio U, Papa M, Perrone-Capano C, Laviola G (2009) Methylphenidate to adolescent rats drives enduring changes of accumbal Htr7 expression: implications for impulsive behavior and neuronal morphology. Genes Brain Behav 8:356–368
Leopoldo M, Lacivita E, Berardi F, Perrone R, Hedlund PB (2011) Serotonin 5-HT7 receptor agents: Structure-activity relationships and potential therapeutic applications in central nervous system disorders. Pharmacol Ther 129:120–148
Maletic-Savatic M, Malinow R, Svoboda K (1999) Rapid dendritic morphogenesis in CA1 hippocampal dendrites induced by synaptic activity. Science 283:1923–1927
Manganas LN, Zhang X, Li Y, Hazel RD, Smith SD, Wagshul ME, Henn F, Benveniste H, Djuric PM, Enikolopov G, Maletic-Savatic M (2007) Magnetic resonance spectroscopy identifies neural progenitor cells in the live human brain. Science 318:980–985
Marco EM, Adriani W, Canese R, Podo F, Viveros MP, Laviola G (2007) Enhancement of endocannabinoid signalling during adolescence: Modulation of impulsivity and long-term consequences on metabolic brain parameters in early maternally deprived rats. Pharmacol Biochem Behav 86:334–345
Meneses A, Perez-Garcia G, Liy-Salmeron G, Flores-Galvez D, Castillo C, Castillo E (2008) The effects of the 5-HT(6) receptor agonist EMD and the 5-HT(7) receptor agonist AS19 on memory formation. Behav Brain Res 195:112–119
Meneses A (2014) 5-HT7 receptor stimulation and blockade: a therapeutic paradox about memory formation and amnesia. Front Behav Neurosci 8:207
Mukherjee P, McKinstry RC (2006) Diffusion tensor imaging and tractography of human brain development. Neuroimaging Clin N Am 16:19–43, vii
Noll DC, Genovese CR, Nystrom LE, Vazquez AL, Forman SD, Eddy WF, Cohen JD (1997) Estimating test-retest reliability in functional MR imaging. II: Application to motor and cognitive activation studies. Magn Reson Med 38:508–517
Pajevic S, Pierpaoli C (1999) Color schemes to represent the orientation of anisotropic tissues from diffusion tensor data: application to white matter fiber tract mapping in the human brain. Magn Reson Med 42:526–540
Pan WJ, Thompson G, Magnuson M, Majeed W, Jaeger D, Keilholz S (2011) Broadband local field potentials correlate with spontaneous fluctuations in functional magnetic resonance imaging signals in the rat somatosensory cortex under isoflurane anesthesia. Brain Connect 1:119–131
Pawela CP, Biswal BB, Cho YR, Kao DS, Li R, Jones SR, Schulte ML, Matloub HS, Hudetz AG, Hyde JS (2008) Resting-state functional connectivity of the rat brain. Magn Reson Med 59:1021–1029
Pawela CP, Biswal BB, Hudetz AG, Schulte ML, Li R, Jones SR, Cho YR, Matloub HS, Hyde JS (2009) A protocol for use of medetomidine anesthesia in rats for extended studies using task-induced BOLD contrast and resting-state functional connectivity. Neuroimage 46:1137–1147
Paxinos G, Watson C (1998) The Rat Brain in Streotaxic Coordinates. Academic Press, Inc
Perez-Garcia GS, Meneses A (2005) Effects of the potential 5-HT7 receptor agonist AS 19 in an autoshaping learning task. Behav Brain Res 163:136–140
Perez-Garcia G, Meneses A (2009) Memory time-course: mRNA 5-HT1A and 5-HT7 receptors. Behav Brain Res 202:102–113
Porsolt RD, Le Pichon M, Jalfre M (1977) Depression: a new animal model sensitive to antidepressant treatments. Nature 266:730–732
Prince CR, Collins C, Anisman H (1986) Stressor-provoked response patterns in a swim task: modification by diazepam. Pharmacol Biochem Behav 24:323–328
Provencher SW (1993) Estimation of metabolite concentrations from localized in-vivo proton NMR spectra. Magn Reson Med 30:672–679
Raichle ME, Snyder AZ (2007) A default mode of brain function: a brief history of an evolving idea. Neuroimage 37:1083–1090, discussion 1097-9
Razafsha M, Behforuzi H, Harati H, Wafai RA, Khaku A, Mondello S, Gold MS, Kobeissy FH (2013) An updated overview of animal models in neuropsychiatry. Neuroscience 240:204–218
Renner U, Zeug A, Woehler A, Niebert M, Dityatev A, Dityateva G, Gorinski N, Guseva D, Abdel-Galil D, Fröhlich M, Döring F, Wischmeyer E, Richter DW, Neher E, Ponimaskin EG (2012) Heterodimerization of serotonin receptors 5-HT1A and 5-HT7 differentially regulates receptor signalling and trafficking. J Cell Sci 125(Pt 10):2486–2499
Robinson TE, Kolb B (1997) Persistent structural modifications in nucleus accumbens and prefrontal cortex neurons produced by previous experience with amphetamine. J Neurosci 17:8491–8497
Romano E, Ruocco LA, Nativo P, Lacivita E, Ajmone-Cat MA, Boatto G, Nieddu M, Tino A, Sadile AG, Passarelli F, Leopoldo M, Laviola G, Adriani W (2014) Effects of Subchronic Lp-211, a New 5-HT7-r Agonist, on Adult Behaviour in Mice and Rats. Review in the Neurosciences, in press
Ruocco LA, Treno C, Gironi Carnevale UA, Arra C, Boatto G, Nieddu M, Pagano C, Illiano P, Barbato F, Tino A, Carboni E, Laviola G, Lacivita E, Leopoldo M, Adriani W, Sadile AG (2014a) Prepuberal Stimulation of 5-HT7-R by LP-211 in a Rat Model of Hyper-Activity and Attention-Deficit: Permanent Effects on Attention, Brain Amino Acids and Synaptic Markers in the Fronto-Striatal Interface. PLoS ONE 9:e83003
Ruocco LA, Romano E, Treno C, Lacivita E, Arra C, Gironi-Carnevale UA, Travaglini D, Leopoldo M, Laviola G, Sadile AG, Adriani W (2014b) Emotional and risk-seeking behavior after prepuberal subchronic or adult acute stimulation of 5-HT7-Rs in Naples High Excitability rats. Synapse 68:159–167
Sarkisyan G, Hedlund PB (2009) The 5-HT7 receptor is involved in allocentric spatial memory information processing. Behav Brain Res 202:26–31
Schaechter JD, Fricker ZP, Perdue KL, Helmer KG, Vangel MG, Greve DN, Makris N (2009) Microstructural status of ipsilesional and contralesional corticospinal tract correlates with motor skill in chronic stroke patients. Hum Brain Mapp 30:3461–3474
Sholl DA (1981) The organization of the cerebral cortex. Methuen, Methuen
Song SK, Sun SW, Ramsbottom MJ, Chang C, Russell J, Cross AH (2002) Dysmyelination revealed through MRI as increased radial (but unchanged axial) diffusion of water. Neuroimage 17:1429–1436
Speranza L, Chambery A, Di Domenico M, Crispino M, Severino V, Volpicelli F, Leopoldo M, Bellenchi GC, di Porzio U, Perrone-Capano C (2013) The serotonin receptor 7 promotes neurite outgrowth via ERK and Cdk5 signaling pathways. Neuropharmacology 67:155–167
Sprouse J, Reynolds L, Li X, Braselton J, Schmidt A (2004) 8-OH-DPAT as a 5-HT7 agonist: phase shifts of the circadian biological clock

through increases in cAMP production. Neuropharmacology 46:52–62

Steimer T (2011) Animal models of anxiety disorders in rats and mice: some conceptual issues. Dialogues Clin Neurosci 13: 495–506

Sun SW, Liang HF, Trinkaus K, Cross AH, Armstrong RC, Song SK (2006) Noninvasive detection of cuprizone induced axonal damage and demyelination in the mouse corpus callosum. Magn Reson Med 55:302–308

Takao H, Hayashi N, Ohtomo K (2010) White matter asymmetry in healthy individuals: a diffusion tensor imaging study using tract-based spatial statistics. Neuroscience 193:291–299

Udo H, Jin I, Kim JH, Li HL, Youn T, Hawkins RD, Kandel ER, Bailey CH (2005) Serotonin-induced regulation of the actin network for learning-related synaptic growth requires Cdc42, N-WASP, and PAK in Aplysia sensory neurons. Neuron 45: 887–901

van Praag H, Kempermann G, Gage FH (2000) Neural consequences of environmental enrichment. Nat Rev Neurosci 1:191–198

Vincent JL, Patel GH, Fox MD, Snyder AZ, Baker JT, Van Essen DC, Zempel JM, Snyder LH, Corbetta M, Raichle ME (2007) Intrinsic functional architecture in the anaesthetized monkey brain. Nature 447:83–86

Wang S, Melhem ER (2005) Amyotrophic lateral sclerosis and primary lateral sclerosis: The role of diffusion tensor imaging and other advanced MR-based techniques as objective upper motor neuron markers. Ann N Y Acad Sci 1064:61–77

Waters KA, Stean TO, Hammond B, Virley DJ, Upton N, Kew JN, Hussain I (2012) Effects of the selective 5-HT(7) receptor antagonist SB-269970 in animal models of psychosis and cognition. Behav Brain Res 228:211–218

Wesolowska A, Nikiforuk A, Stachowicz K, Tatarczynska E (2006) Effect of the selective 5-HT7 receptor antagonist SB 269970 in animal models of anxiety and depression. Neuropharmacology 51: 578–586

Wilson DA, Hoptman MJ, Gerum SV, Guilfoyle DN (2011) State-dependent functional connectivity of rat olfactory system assessed by fMRI. Neurosci Lett 497:69–73

Withers GS, Greenough WT (1989) Reach training selectively alters dendritic branching in subpopulations of layer II-III pyramids in rat motor-somatosensory forelimb cortex. Neuropsychologia 27:61–69

Zoratto F, Tringle AL, Bellenchi G, Speranza L, Travaglini D, di Porzio U, Perrone-Capano C, Laviola G, Dreyer JL, Adriani W (2013) Impulsivity and home-cage activity are decreased by lentivirus-mediated silencing of serotonin transporter in the rat hippocampus. Neurosci Lett 548:38–43